belonging to the hematite–quartz series, to those obtained with the internal standard method. We added 20% of lithium fluoride (internal standard) to those samples. The homogeneity of the samples were obtained by mixing the samples and the internal standard for 30 min in a mill of agate. The measurements of the intensities of the reflection peaks for quartz and hematite were performed under the same experimental conditions as those described above. For the LiF internal standard we used the (200) reflection and the intensity was integrated with an angular speed of 0.5° per minute. In Table V we quoted the values of I_q/I_s and I_h/I_s, where I_q, I_h, and I_s are the diffracted integrated intensities of quartz, hematite, and internal standard, respectively. In the same table are reported the concentrations computed from I_q/I_s and I_h/I_s with a least squares method program.

CONCLUSIONS

Comparing the values of Table I to the corresponding values of Table V we can deduce that the proposed method gives a better agreement between the experimental and theoretical data. It permits the recovering of the samples and the analysis of material containing many crystalline phases avoiding eventual overlapping between reflections belonging to the internal standard and to the crystalline phase being analyzed. However the proposed method requires a measurement of the intensity of the Ag Kα Compton scattered radiation and therefore the use of an x-ray spectrometer.

In conclusion, when the chemical composition is such that the proposed method may be used, this method is to be preferred for its greater precision and the simplicity of the manual operations involved.

LITERATURE CITED

(1) H. P. Klug and L. Alexander, "X-Ray Diffraction Procedures for Polycrystalline and Amorphous Materials", New York, John Wiley & Sons, 1954, p 415.
(2) M. Franzini, L. Leoni, and M. Saitta, *X-Ray Spectrom.*, **5**, 84 (1976).
(3) M. Franzini, L. Leoni, and M. Saitta, *Rend. Soc. Ital. Mineral. Petrol.*, **31** (2), 365 (1975).
(4) M. Franzini, L. Leoni, and M. Saitta, *X-Ray Spectrom.*, **5**, 208 (1976).
(5) R. Jenkins and J. L. De Vries, "Practical X-Ray Spectrometry", Philips Technical Library, 1967.

RECEIVED for review January 21, 1977. Accepted April 5, 1977.

Performance of a Silicon Target Vidicon Tube as a Multiwavelength Detector for Liquid Chromatography

Alan E. McDowell and Harry L. Pardue*

Department of Chemistry, Purdue University, West Lafayette, Indiana 47907

Performance characteristics and unique applications of a silicon target vidicon tube as a multiwavelength detector for liquid chromatography are discussed and compared with a commercially available system. For the spectral range from about 200 nm to above 800 nm, the device permits scan repetition rates up to 100 scans per second and has a linear dynamic range of at least four orders of magnitude. Noise levels and detection limits are comparable to a commercial system. Special applications include selection of optimal wavelengths, detection of interferences, and quantitative resolution of overlapping chromatographic peaks.

The advantages and limitations of liquid chromatography (LC) as an analytical tool for complex samples are well documented (*1*) and need not be reviewed here. This separation method, like any other, requires a sensitive and versatile detector to be used most effectively. Detection methods based upon the absorption or emission of radiant energy have been most popular in the recent past (*2*). While both single and variable wavelength detectors are available, most commercial instruments have utilized single wavelength or manually operated variable wavelength systems.

Several reports in the recent literature have described applications of rapid scanning spectrometers as detectors for LC. Denton et al. (*3*) used an oscillating mirror rapid scanning instrument as an LC detector. Dessy et al. (*4*, *5*) have suggested the use of solid state diode arrays as LC detectors and Milano et al. (*6*) have reported performance data for such a detector system. These reports suggest that integrating array detectors, which can improve the signal to noise ratio by virtue of the multichannel advantage, show favorable potential for use as rapid scanning multiwavelength LC detectors. A correspondence from this laboratory (*7*) described the application of a silicon target vidicon tube as a multiwavelength detector for LC. This report describes the system and its performance characteristics in more detail and discusses some applications illustrating advantages of multiwavelength detectors in general.

EXPERIMENTAL

Vidicon Spectrometer. The rapid scanning spectrometer used in this work was based on a silicon diode array vidicon camera tube (No. 4532/F RCA, Lancaster, Pa. 17604) and a magnetic focus and deflection assembly (No. CY100-1465, Penn-Tran Corporation, Bellefonte, Pa. 16823). The associated electronics used to operate the vidicon tube, provide the deflection waveforms and process the signal, and the on-line minicomputer data acquisition system have been described previously (*8*, *9*).

Chromatographic System. A Milton Roy Instrument mini Pump (No. 396-31, Laboratory Data Control, Riviera Beach, Fla. 33404) was used to pump eluent to an Altex 2 mm × 500 mm glass microbore column (No. 251-02, the Anspec Company Inc., Ann Arbor, Mich. 48107) packed with Vydac anion-exchange resin with a 30–44 μm particle size distribution (No. 900-05, Anspec). Samples were injected using an Altex septum injector (No. 251-12, Anspec). Column pressures of 400–500 psi were monitored prior to the injector with a 0–1000 psi pressure gauge (No. 904-1, Anspec) at flow rates of 0.4–0.5 mL/min. Connections were made using Altex Teflon fittings and tubing. The pump, pressure gauge, injector, and column were mounted on a column and pump stand (No. CS-1, Bioanalytical Laboratories, West Lafayette, Ind. 47906). Eluents were degassed by heating to 60 °C and held at 30–40 °C during operation.

Flow-Cell and Optical System. The flow cell from an Aminco Morrow stopped flow mixing system (No. B30-68109, American

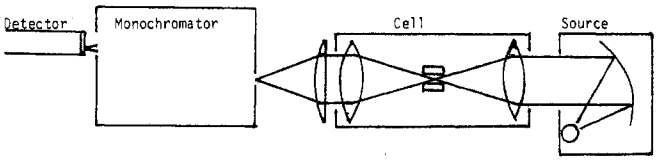

Figure 1. Schematic representation of optical system

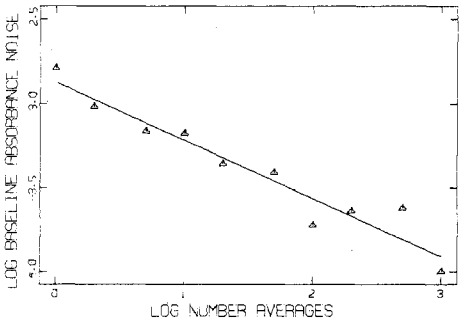

Figure 2. Effect of ensemble averaging on baseline noise

Instrument Co., Silver Spring, Md. 20910) modified by replacing the Teflon input chamber by a Teflon exhaust chamber, was used as the observation cell. The cell has a path length of 1 cm and a volume of 32 mL. The output from a 20-W deuterium source (source No. 9780 and supply No. 71701, Beckman Instruments, Inc., Fullerton, Calif. 92634) is focused through the cell using 1-in. diameter UV grade condensing lenses with a 2-in. focal length and focused onto the entrance slit of a monochromator (No. 33-86-25, Bausch and Lomb, Rochester, N.Y. 14602) with a 1-in. diameter cylindrical lens with a $1^1/_2$-in. focal length (Lenses were obtained from Esco Optics Products, Oak Ridge, N.J. 07438). The grating used in the monochromator was blazed at 200 nm with 600 grooves/mm (No. 35-53-04-050, Bausch and Lomb) allowing a 200-nm wavelength range to be dispersed across the vidicon target placed in the exist focal plane. Figure 1 is a schematic representation of the optical system.

Reagents. Buffers were prepared using reagent grade chemicals. Acetaminophen, caffeine, ephedrine–HCl, phenobarbital, phenylpropanolamine–HCl, and uric acid were obtained from Sigma Chemical Co., St. Louis, Mo. 63178. Theophylline was supplied compliments of Lilly Research Laboratories, Indianapolis, Ind. 46206.

RESULTS AND DISCUSSION

Detector Performance. Important characteristics of this or any other detector include electrical noise, spectral response, and dynamic range. Each of these items is discussed below for the vidicon system described above.

System Noise. Several experiments were performed to evaluate the noise characteristics of the vidicon system. In one set of experiments, the absorbance of an empty cell was monitored at 245 nm at a frequency of 100 Hz. Starting at 10-s intervals during a 43-min period, different numbers (1 to 1000) of measurements were made, the results for each data set were averaged, and the baseline absorbance noise was evaluated. Figure 2 represents a log–log plot of noise vs. the number of points averaged. The noise falls from a value of 0.0015 absorbance unit for only one point to a value of 0.0001 absorbance unit for 1000 points averaged. For random noise, the slope of the log–log plot should be −0.5; however the least squares slope of these data is −0.35 ± 0.03, suggesting a nonrandom component to the noise. Also, for more than 100 points included in the average, the improvement in the noise figure is unpredictable. Accordingly, in all of the data presented below, each point represents the average of 100 points taken during a 1-s period.

The origin of the nonrandom noise component is apparent in Figure 3A in which 125 alternate points of a total of 250 points (100 averages per point) taken at 215 nm over a period of 43 min are plotted as a function of time. The signal is

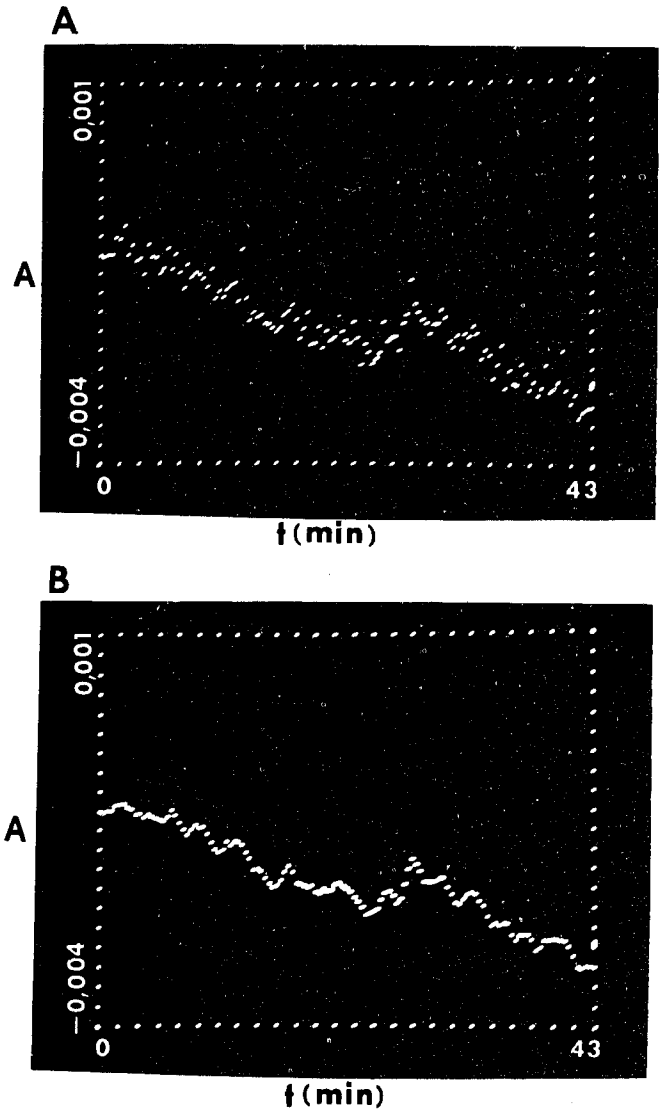

Figure 3. Baseline at 215 nm. (A) Before numerical smoothing. (B) After smoothing

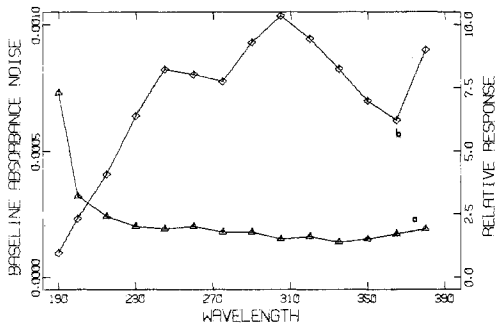

Figure 4. Baseline noise (a) and relative system response (b) as a function of wavelength

observed to drift by an observable amount during the 43-min period. The drift, which is probably source drift, is about 0.003 absorbance unit (AU) per hour. Figure 3B illustrates the effect of a 13-point smooth (*10*) using all 250 data points. This smoothing step reduces the noise from 0.00024 AU to 0.00019 AU.

The relative spectral response for the system and the baseline noise at different wavelengths are included in Figure 4. The system is observed to give measurable response below 200 nm. The baseline noise is about 0.0007 AU at 190 nm and decreases to about 0.0002 AU for wavelengths above about 210 nm. Baseline noise is dependent on spectral response in

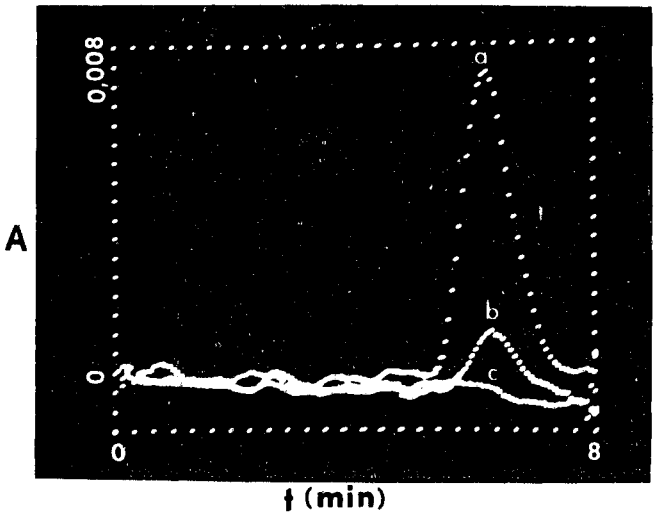

Figure 5. Chromatograms for uric acid at 293 nm. Samples containing 50 ng (a), 10 ng (b), and 1 ng (c)

that quantization error and the relatively constant random electrical noise become more important for lower signals. Measures which tend to flatten the system response will allow baseline noise to be about the same at all wavelengths. Alternatively, an autoranging amplifier which would provide higher gain for smaller signals or variable integration periods could be used to improve the baseline signal to noise ratio.

Dynamic Range. Uric acid was used as an example system to evaluate the quantitative performance of the detector system for a chromatographic peak. Figure 5 represents chromatograms (absorbance at 293 nm) for 10 μL samples containing 1, 10 and 50 ng of uric acid eluted from a column with pH 4.75, 0.05 M acetate buffer. The baseline error at this wavelength expressed as the standard error about a line fit to the data of a blank injection, was 0.0002 AU. The absorbance at 293 nm was smoothed and integrated by summing absorbances throughout the peak and correcting for baseline area. The regression equation for area vs. concentration is $y = (0.04303 \pm 0.00013)X + 0.0008 \pm 0.04$, and the standard error of estimate and correlation coefficient are 0.127 and 0.9999, respectively. The area for the 0.1 mg/L sample which is equivalent to 1 ng of uric acid was 0.0045 area unit, while the value for a blank was 0.001 area unit. Thus the detection limit for uric acid is in the range of 1 ng for this system.

Comparison with Commercial Instrument. Data presented above are summarized in Table I along with manufacturer's specifications for a commercially available instrument for comparison purposes. The most obvious differences are the scan rate where the vidicon system has a pronounced advantage and the photometric drift where the commercial instrument has a pronounced advantage. The large drift figure for the vidicon system results from the fact that it is a single beam instrument. We are presently working on methods to reduce this problem. The resolution quoted for the vidicon system is a function of the electronic resolution of the detector (about 200 resolution elements) (*11*) and the characteristics of the dispersion optics, and can be adjusted using different dispersion optics. Baseline noise for the vidicon, given as standard deviations, exceeds that of the commercial instrument, given as peak to peak values, by about a factor of four.

Applications. Some of the principal advantages of multiwavelength detectors have already received attention in the literature (*3–7*). These detectors provide fingerprint spectral identification information to complement retention times and, as such, resemble the use of mass spectrometric

Table I. Comparison of Vidicon and Commercial[a] LC Detector Systems

	Vidicon	LDC Spectro-Monitor II
Flow cell	32 μL single beam	10 μL dual beam
Wavelength range	190–1000 nm	190–690 nm
Bandwidth	5 nm	5 nm
Response time	0.01 s/scan	1–5 s
Noise 210 nm	0.0003 A (100 averages)	0.0003 A
254 nm	0.0002 A	0.0002 A
280 nm	0.0002 A	0.0002 A
Drift	0.003 A/h	0.0005 A/h

[a] Model 1202, SpectroMonitor II, Laboratory Data Control, Riviera Beach, Fla. 33404.

detection in gas chromatography. They allow selection of wavelengths which optimize sensitivity and resolution for each component in the chromatogram. No single compromise wavelength need be selected. They allow one to tune interferences out of the chromatogram by selecting wavelengths where the response for the interferences is negligible. Both absorbance and the derivative of absorbance with wavelength have been used as the response in this regard.

Other capabilities multiwavelength detectors can offer include the ability to offer useful dynamic range for different components which may be present in very different concentrations or may have very different absorptivities at just one wavelength, the ability to resolve overlapping chromatographic peaks quantitatively, and the ability to detect impurities in chromatographic peaks. Examples reported below have been selected to illustrate both the quantitative performance of the system and some special types of applications simultaneously.

Uncertainties in the regression equations are expressed as standard deviation units ($X \pm 1S$).

Acetaminophen and Phenylpropanolamine–HCl. The pharmaceutical preparation Sinutab II contains about 325 mg of acetaminophen (AAP) and 25 mg of phenylpropanolamine–HCl (PPA) per tablet. Figure 6A represents a chromatogram monitored at 245 nm of a 5-μL injection of the above amounts of these species in 100 mL of pH 9 buffer. The larger peak corresponds to AAP with a retention time of 6.0 min and the smaller peak corresponds to PPA with a retention time of 2.8 min. The concentration and absorptivity differences are such that the absorbance areas differ by a factor of 800 at 254 nm, making it difficult to perform reliable determinations of both components at a single instrument setting at this one wavelength.

Figure 6B represents the spectra for these components which show that better sensitivity for PPA can be obtained at 210 nm, and that a somewhat longer wavelength such as 320 nm can be used to keep the AAP absorbance in a more suitable range. Figure 6C shows chromatograms at these wavelengths (210 nm and 320 nm) for a single Sinutab II tablet crushed, equilibrated with pH 9 buffer for 10 min, filtered, and diluted to 100 mL with pH 9 buffer. Peaks due to both components are observed at 210 nm but only one peak for AAP is observed at 320 nm, and the smaller peaks permit the same instrument settings to be used for both components.

Regression of area (y) at these wavelengths vs. concentration (x mg/100 mL) in aqueous preparations yielded for AAP $y = (0.00443 \pm 0.0006)x \pm (0.0553 \pm 0.0264)$, a standard error of estimate of 0.037 and a correlation coefficient of 0.999, and for PPA $y = (0.0590 \pm 0.0008)x \pm (0.013 \pm 0.0260)$, a standard error of estimate of 0.037 and a correlation coefficient of 0.999. Analysis of nine different Sinutab II tablets gave 25.17 ± 0.6 mg of PPA and 333.5 ± 9.6 mg of AAP corresponding to

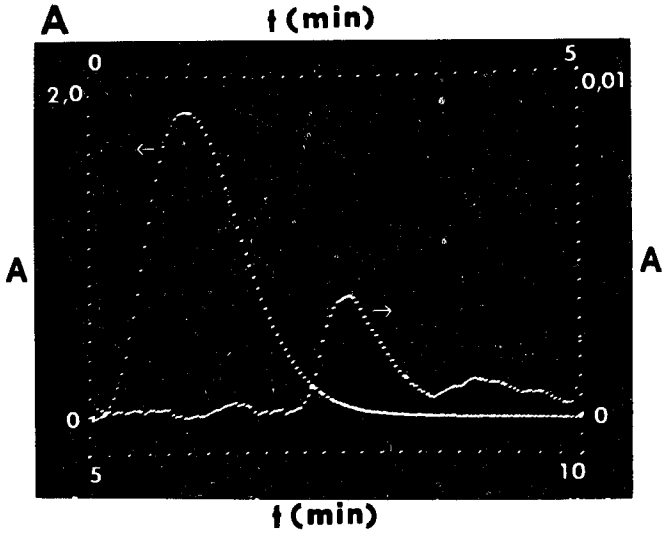

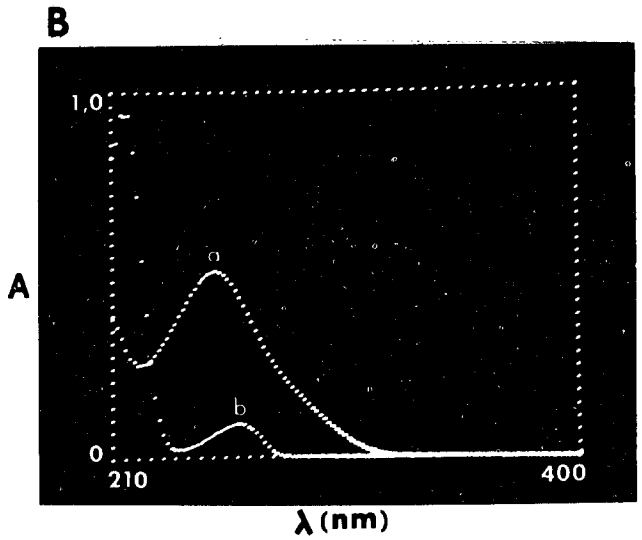

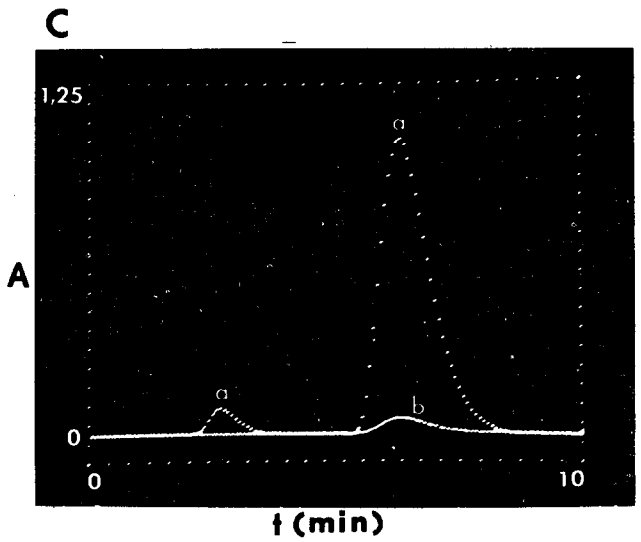

Figure 6. Chromatographic and spectral data for Sinutab II components. (A) Chromatogram of 16.2 μg AAP and 1.25 μg PPA at 254 nm. (B) Spectra of AAP 9 mg/L (a) and PPA 109 mg/L (b). (C) Chromatograms of Sinutab II tablet extract at 210 nm (a) and 320 nm (b)

100.7% and 102.6% recoveries with standard errors of 2.3% and 3.0%, respectively, based upon manufacturers' stated values.

Ephedrine–HCl Theophylline, and Phenobarbital. Primatene tablets contain ephedrine-HCl (EPD), theophylline (TPH), and phenobarbital (PBT) at the nominal levels 24, 130, and 8 mg, respectively. Figure 7 represents a chromatogram monitored at 220 nm of a Primatene tablet extract eluted from a column with pH 8 buffer. Analysis of Primatene tablets yielded results for EPH which were significantly higher than expected on the basis of stated values. We suspected the high results were due to an interfering component being eluted with the EPH and used the multiwavelength capability of the vidicon based detector to confirm this suspicion.

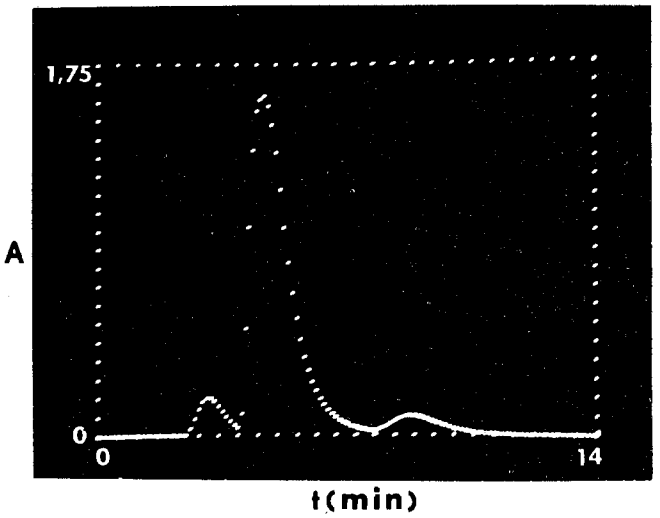

Figure 7. Chromatogram at 220 nm of Primatene tablet extract containing, in order of elution, EPD, TPH, and PBT

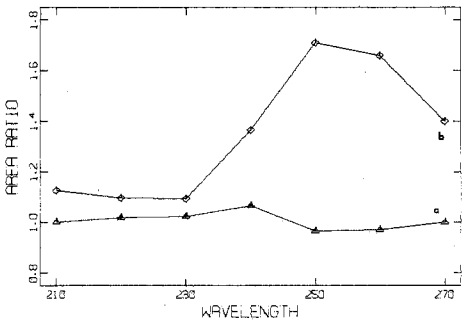

Figure 8. Area ratio plot showing interference with ephedrine in Primatene extract. Comparison of ephedrine standard vs. ephedrine standard (a) and ephedrine peak from Primatene extract vs. standard at concentration equivalent to extract with nominal tablet contents (b)

If it is assumed that the area for component n at a given wavelength ($A_{n,\lambda}$) is proportional to the concentration (C_n) of that component,

$$A_{n,\lambda} = K_{n,\lambda} C_n \tag{1}$$

and if one compares the areas for a pure reference ($A_{R,\lambda}$) and an unknown ($A_{u,\lambda}$) where the unknown may contain two or more components, then it is easily shown that the ratio of areas at a given wavelength is given by

$$\frac{A_{u,\lambda}}{A_{R,\lambda}} = \frac{C_{1,u}}{C_{1,R}} + \frac{K_{2,\lambda}}{K_{1,\lambda}} \times \frac{C_{2,u}}{C_{1,R}} \tag{2}$$

where the subscripts 1 and 2 refer to the analyte and suspected interference, respectively. For a single experiment, the concentration ratios are constant, but the proportionality constants (K_1 and K_2) will vary with wavelength in proportion to the effective absorptivities for the components. If there is no interference in the sample ($C_{2,u} = 0$), then a plot of the ratio, $A_{u,\lambda}/A_{R,\lambda}$ vs. wavelength should give a horizontal line subject only to experimental error. On the other hand, if there is an interference present with spectral properties different from the analyte, then the plot of $A_{u,\lambda}/A_{R,\lambda}$ vs. wavelength

would be expected to reflect these spectral differences.

Figure 8 represents plots of the area ratios for two standards (curve a) and an unknown and a standard (curve b). It is observed that the variation in the unknown is much greater than the experimental uncertainty reflected by the standards plot. These data confirm the presence of an interference in the EPH peak and illustrate another useful application of the multiwavelength data. The interference is most probably a basic dye which elutes with the EPH which is also basic and as such was not retained on the column used in this work.

The shape of the plot in Figure 8 can provide additional information about this system. Because, for a given run, the concentration ratios in Equation 2 are constant, it follows that the maxima and minima in the plot must correspond to points where the ratios of proportionality constants have maximum and minimum values. Because the relative contribution of a contaminant to computed analyte concentration will be a minimum when $K_{2,\lambda}/K_{1,\lambda}$ is a minimum, this plot could provide some guidance in the selection of the best wavelength to minimize interferences.

What we have presented here is just one example of how multiwavelength data can be used to detect the presence of an interference. If, instead of using ratios of areas, one used ratios of absorbance at different points in time throughout the peak, then it would be possible to determine the extent of overlap of two partially separated components. Also, appropriate treatment of absorbance data can provide statistical information which can be used in standard statistical tests to suggest the degree of confidence with which the presence of an interference is predicted. If interferences are not exactly overlapped with the component of interest, more information as to the number of interferences and the nature of their spectra can be deduced from spectral changes that occur throughout the overlapped peaks (*12*). A more detailed analysis of the advantages and limitations of these different approaches will be discussed in a later paper.

For this situation in which the spectral properties of the unknown are not known, one can only hope to determine if an interference is or is not present. However, if the spectral properties of all components in a single peak or a pair of overlapped peaks are known, then it is possible to use multiwavelength data to resolve these components quantitatively as discussed in the next section.

Acetaminophen and Caffeine. Acetaminophen (AAP) and caffeine (CAF) were run under chromatographic conditions such that their chromatographic peaks overlapped badly and multiwavelength data were used to resolve the overlapped peaks quantatively. The top curve in Figure 9B represents a chromatogram monitored at 254 nm of a 10 μL injection of a solution containing 25 mg/L each of both components. The overlap is such that quantitation by conventional methods would be difficult at best.

Figure 9B represents the spectra for the individual components. Although there is overlap at all wavelengths, there are significant differences between the spectra and these differences are exploited to resolve the components quantitatively. One recent report described the use of separate detectors to resolve overlapped peaks (*13*) while another report described the use of a vidicon based spectrometer to resolve mixtures containing up to seven components (*14*). The latter approach was used in this work.

The approach involves the prior determination of absorptivities at several wavelengths for the pure components and using these absorptivities and sample absorbances in matrix equations to solve for the concentrations of the individual components. We used five standards to determine absorptivities at 246, 251, 259, 267, and 275 nm. Absorbance values at these same wavelengths were then used to compute

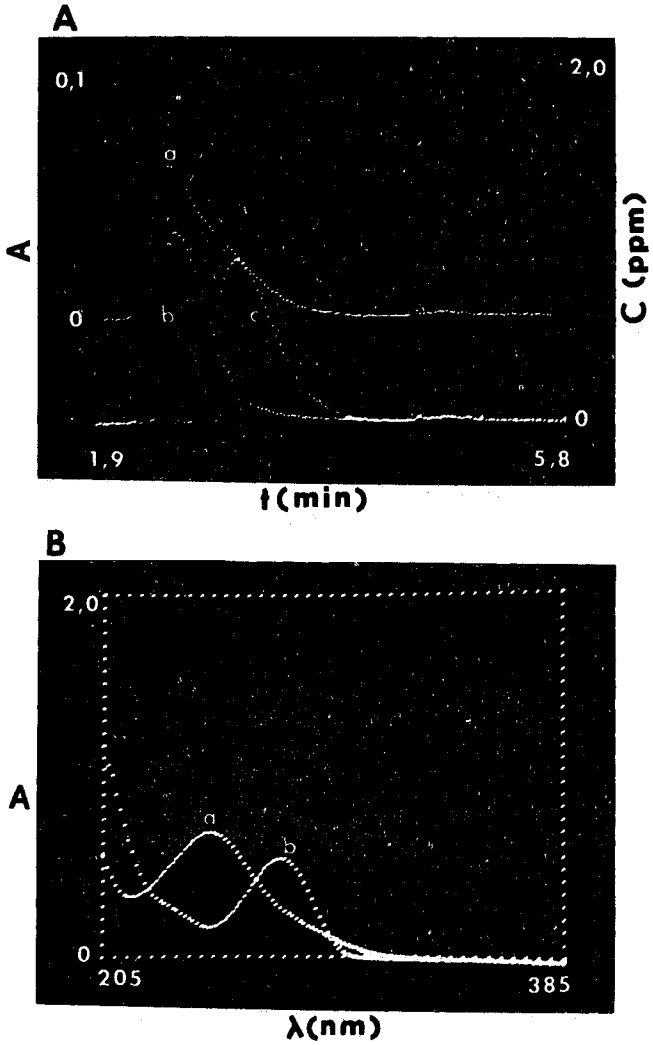

Figure 9. Chromatographic and spectral data for AAP and CAF. (A.) Chromatogram of mixture of AAP and CAF, 25 mg/L each, at 254 nm (a), chromatograms after deconvolution for AAP (b) and CAF (c). (B.) Spectra of AAP 5 mg/L (a) and CAF 5 mg/L (b)

the concentration of each component at each point in time throughout the chromatogram. The lower curves in Figure 9A represent the deconvoluted peaks for the mixture represented by the top curve. The first peak with a retention time of 2.5 min represents AAP and the second peak with a retention time of 3.1 min represents CAF. Concentrations of components in the sample were computed from the equation

$$C_S = \frac{\left(\sum_{i=1}^{n} C_i\right) \times FR \times DR}{SS} \qquad (3)$$

where FR is the flow rate, DR is the time between successive data points, and SS is the sample injection volume.

Results were obtained with this procedure for ten aqueous mixtures of the two components. Regression equations of found (y) vs. added (x) amounts were $y = (1.007 \pm 0.021)X \pm (0.2 \pm 0.6)$ mg/L and a standard error of estimate and correlation coefficient of 1.0 mg/L and 0.998 for AAP and $y = (1.019 \pm 0.017)X - (0.3 \pm 0.5)$ mg/L with a standard error of estimate and correlation coefficient of 0.8 mg/L and 0.999 for CAF. These data are comparable to those obtained for well resolved chromatographic peaks and demonstrate another dimension for multiwavelength detectors.

The computational procedure used here is similar to that suggested previously (*13*), but has the advantage that it is not

necessary to chromatograph the standards if the flow rate is known. Also, information in the time domain is retained.

Projections. The most serious limitation of the vidicon detector system used in this work is the photometric drift which results from the single beam operation and we now have work under way designed to provide double beam operation with a stabilized source. This can be achieved using a single detector and one set of dispersion optics and thus shows an advantage over linear diode array detectors where two matched detectors and two sets of dispersion optics are necessary for double beam operation. Another less critical limitation is that some tradeoff must be made between spectral range and resolution and we are working on optical systems which will provide both broad coverage and good resolution. Recent work in this laboratory has demonstrated that the use of integrated area under an absorption profile can improve photometric precision in comparison with single wavelength data (*9*). We have work under way to determine if this technique offers any significant advantage for chromatographic processes. The vidicon detector offers a convenient approach for derivative spectroscopy (*15*, *16*) and there may be useful applications of derivative spectra for liquid chromatography. Finally, although this paper has emphasized the absorption process, vidicon detectors can also be used as fluorescence detectors (*17*), and multiwavelength fluorescence detection should offer real advantages in liquid chromatography.

We conclude from this work that the silicon target vidicon is a viable multiwavelength detector for liquid chromatography, that it offers several potential advantages over single wavelength detectors, and that there still are several aspects of the concept which merit attention.

LITERATURE CITED

(1) L. R. Snyder and J. J. Kirkland, "Introduction to Modern Liquid Chromatography", John Wiley and Sons, New York, N.Y., 1974.
(2) H. M. McNair, *J. Chromatogr. Sci.*, **14**, 477 (1976).
(3) M. S. Denton, T. P. DeAngelis, A. M. Yacynych, W. R. Heineman, and T. W. Gilbert, *Anal. Chem.*, **48**, 20 (1976).
(4) R. E. Dessy, W. G. Nunn, C. A. Titus, and W. R. Reynolds, *J. Chromatogr. Sci.*, **14**, 195 (1976).
(5) R. E. Dessy, W. D. Reynolds, W. G. Nunn, C. A. Titus, and G. F. Molar, *Clin. Chem. (Winston-Salem, N.C.)*, **22**, 1472 (1976).
(6) M. J. Milano, S. Lam, and E. Grushka, *J. Chromatogr.*, **125**, 315 (1976).
(7) A. E. McDowell and H. L. Pardue *Anal. Chem.*, **48**, 1815 (1976).
(8) M. J. Milano, H. L. Pardue, T. E. Cook, R. E. Santini, D. W. Margerum, and J. M. T. Raycheba, *Anal. Chem.*, **46**, 374 (1974).
(9) H. L. Felkel and H. L. Pardue, *Anal. Chem.*, in press.
(10) A. Savitzky and M. J. E. Golay, *Anal. Chem.*, **36**, 1627 (1964).
(11) T. A. Nieman and C. G. Enke, *Anal. Chem.*, **48**, 619 (1976).
(12) W. H. Lawton and E. A. Sylvestre, *Technometrics*, **13**, 617 (1976).
(13) R. G. Berg, C. Y. Ko, J. M. Clemons, and H. M. McNair, *Anal. Chem.*, **47**, 2480 (1975).
(14) A. E. McDowell, R. S. Harner, and H. L. Pardue, *Clin. Chem. (Winston-Salem, N.C.)*, **22**, 1862 (1976).
(15) T. E. Cook, R. E. Santini, and H. L. Pardue, *Anal. Chem.*, **48**, 451 (1976).
(16) T. E. Cook, R. E. Santini, and H. L. Pardue, *Anal. Chem.*, in press.
(17) I. M. Warner, J. B. Callis, E. R. Davidson, and G. D. Christian, *Clin. Chem. (Winston-Salem, N.C.)*, **22**, 1483 (1976).

RECEIVED for review March 3, 1977. Accepted April 29, 1977. This investigation was supported in part by PHS Research Grant No. GM 13326-10 and 11 from the National Institutes of Health.

Determination of Anions in Boiler Blow-Down Water with Ion Chromatography

Timothy S. Stevens* and Virgil T. Turkelson

Dow Chemical, U.S.A. Michigan Division Analytical Labs, 574 Bldg., Midland, Michigan 48640

William R. Albe

Dow Chemical, U.S.A., Instrument Applications and Communications, 1603 Bldg., Midland, Michigan 48640

An application of ion chromatography to the analysis of boiler blow-down water is described. Glycolate (produced by decomposition of EDTA), chloride, sulfite, sulfate, and orthophosphate are separated and quantified. The data are used to monitor boiler feedwater treatment. The analytical columns required have a life expectancy of more than one month when employed in an on-line analyzer.

Industrial boilers used for process steam and electrical power generation may require periodic and costly overhaul because of corrosion and scale buildup in boiler tubes. These problems are controlled by chemical treatment of the demineralized and deaerated boiler feedwater and by continuous "blow-down" of the boilers, i.e., a small fraction of the feedwater is not boiled to steam but is continuously drained from the boiler as blow-down water. Monitoring the concentration of the treatment chemicals is needed and this can be done by analyzing the blow-down water.

Ethylenediaminetetraacetic acid (EDTA) and orthophosphate are added to sequester scale-forming calcium and magnesium ions. The orthophosphate added has the additional effect of passivating the boiler tube surface against general overall corrosion. Sodium sulfite treatment scavanges residual oxygen from the boiler water, preventing pitting corrosion. Finally, corrosion caused by hydrogen ion is controlled by adding sodium hydroxide. The reader is referred to (*1*) for a more detailed discussion of boiler water treatment.

In our boiler blow-down water, sulfite concentration is maintained between 5 and 10 ppm as Na_2SO_3. Orthophosphate concentration is maintained between 10 and 20 ppm as Na_2HPO_4. Hydrogen ion concentration is controlled by maintaining the pH at 10.

EDTA treatment is accomplished by continuous feed at the same rate from day to day. Although EDTA is added to the feedwater, it is not detected in blow-down water. However, glycolic acid is detected (confirmed using NMR) and its presence suggests that in the high temperature and pressure of the boiler (~1100 psig) the EDTA hydrolyzes to glycolic